

On the matrices in B-spline collocation methods for Riesz fractional equations and their spectral properties

Mariarosa Mazza¹ | Marco Donatelli¹ | Carla Manni² | Hendrik Speleers²

¹Department of Science and High Technology, University of Insubria, Via Valleggio 11, Como, 22100, Italy

²Department of Mathematics, University of Rome Tor Vergata, Via della Ricerca Scientifica 1, Rome, 00133, Italy

Correspondence

Mariarosa Mazza, University of Insubria, Italy.

Email: mariarosa.mazza@uninsubria.it

Funding information

Beyond Borders Program of the University of Rome Tor Vergata, Grant/Award Number: CUP E84I19002250005; MIUR Excellence Department project awarded to the Department of Mathematics, University of Rome Tor Vergata, Grant/Award Number: CUP E83C18000100006

Abstract

In this work, we focus on a fractional differential equation in Riesz form discretized by a polynomial B-spline collocation method. For an arbitrary polynomial degree p , we show that the resulting coefficient matrices possess a Toeplitz-like structure. We investigate their spectral properties via their symbol and we prove that, like for second order differential problems, the given matrices are ill-conditioned both in the low and high frequencies for large p . More precisely, in the fractional scenario the symbol vanishes at 0 with order α , the fractional derivative order that ranges from 1 to 2, and it decays exponentially to zero at π for increasing p at a rate that becomes faster as α approaches 1. This translates into a mitigated conditioning in the low frequencies and into a deterioration in the high frequencies when compared to second order problems. Furthermore, the derivation of the symbol reveals another similarity of our problem with a classical diffusion problem. Since the entries of the coefficient matrices are defined as evaluations of fractional derivatives of the B-spline basis at the collocation points, we are able to express the central entries of the coefficient matrix as inner products of two fractional derivatives of cardinal B-splines. Finally, we perform a numerical study of the approximation behavior of polynomial B-spline collocation. This study suggests that, in line with non-fractional diffusion problems, the approximation order for smooth solutions in the fractional case is $p + 2 - \alpha$ for even p , and $p + 1 - \alpha$ for odd p .

KEYWORDS

B-spline collocation, fractional operators, isogeometric analysis, spectral distribution, Toeplitz matrices

1 | INTRODUCTION

Fractional diffusion equations (FDEs) generalize classical partial differential equations (PDEs). Their recent success is due to the nonlocal behavior of fractional operators resulting in an appropriate modeling of anomalous diffusion phenomena that appear in several applicative fields, like imaging or electrophysiology.^{1,2} In particular, a standard diffusion equation can be “fractionalized”, either by replacing the derivative in time with a fractional one whose fractional order ranges from

This is an open access article under the terms of the Creative Commons Attribution License, which permits use, distribution and reproduction in any medium, provided the original work is properly cited.

© 2022 The Authors. *Numerical Linear Algebra with Applications* published by John Wiley & Sons Ltd.

0 to 1, or by introducing a fractional derivative in space with order between 1 and 2. The two approaches can also be combined and lead to similar computational issues.

The improved physical description of the considered phenomenon obtained by “fractionalizing” the derivatives, however, translates into a more challenging numerical treatment of the corresponding discretized problems. Indeed, the evaluation/approximation of a fractional operator is numerically more expensive (and often less stable). Moreover, even when standard local discretization methods are adopted, the nonlocality of the fractional operators causes an absence of sparsity in the discretization matrices. This makes FDEs computationally more demanding than PDEs.

Various numerical discretization methods for FDE problems (e.g., finite differences, finite volumes, finite elements, spectral methods) can be found in the literature. We refer the reader to References 3-10 and references therein. In the case of regular spatial domain subdivisions, the discretization matrices inherit a Toeplitz-like structure from the space-invariant property of the underlying operators that can be exploited for the design of ad hoc iterative schemes of multigrid and preconditioned Krylov type (see, e.g., References 11-16). In the context of finite difference/volume discretizations, we mention the structure preserving preconditioning and the algebraic multigrid methods presented in References 11 and 12. Both strategies are based on the spectral analysis of the coefficient matrices via their symbol, a function that provides an approximation of their eigenvalues/singular values.

A similar symbol-based approach has also been successfully utilized in the context of isogeometric analysis (IgA) using polynomial B-splines for the discretization of integer order differential problems; see, for example, References 17-19. In these papers, the spectral information provided by the symbol has been leveraged for the design of effective preconditioners and fast multigrid/multi-iterative solvers²⁰ whose convergence speed is robust with respect to the mesh size and the spline degree. In the context of IgA, alternative iterative techniques have also been developed; see, for example, References 21 and 22.

The present work aims at uncovering the structure and studying the symbol of the discretization matrices obtained by IgA collocation for FDE problems. As a first step towards the spectral treatment of general differential problems involving fractional diffusion operators, we consider here the following fractional diffusion boundary value problem with absorbing boundary conditions:

$$\begin{cases} \frac{d^\alpha u(x)}{d|x|^\alpha} = s(x), & x \in \Omega, \\ u(x) = 0, & x \in \mathbb{R} \setminus \Omega, \end{cases} \quad (1)$$

where $\Omega := (0, 1)$, $\alpha \in (1, 2)$, and

$$\frac{d^\alpha u(x)}{d|x|^\alpha} := \frac{1}{2 \cos(\pi\alpha/2)} \left({}_0^R D_x^\alpha u(x) + {}_x^R D_1^\alpha u(x) \right)$$

is the so-called Riesz fractional operator, while ${}_0^R D_x^\alpha u(x)$, ${}_x^R D_1^\alpha u(x)$ are the left and right Riemann-Liouville fractional derivatives of u (see Section 2.1 for their definition). More precisely, we are interested in a polynomial B-spline collocation-based discretization of (1) where the so-called Greville abscissae are chosen as collocation points.

Collocation methods are widely utilized in the numerical discretization of differential problems thanks to their computational simplicity with respect to other methods like Galerkin-based schemes. In particular, collocation methods with polynomial splines were applied to fractional problems for the first time in Reference 23 and further developed in Reference 24. Polynomial B-spline bases have been used for solving time-fractional problems in Reference 25 and space-fractional problems in References 26 and 27. Among nonpolynomial spline collocation methods for fractional problems, we mention Reference 28 in which the authors explore the application of fractional B-splines.

Our choice of classical polynomial B-splines is motivated by the fact that, contrarily to their fractional counterpart, they have compact support and naturally fulfill boundary and/or initial conditions. Furthermore, they possess good approximation properties. Seminal results concerning the structure of the quadratic spline collocation matrices can be found in Reference 29. Therein, the authors recognize the Toeplitz-like structure of the coefficient matrices and use a classical circulant preconditioner to solve the corresponding linear systems by means of Krylov methods.

To the best of our knowledge, this is the first time that the structure and the spectral properties of polynomial B-spline collocation matrices are investigated for an arbitrary polynomial degree p . We show that the coefficient matrices retain the Toeplitz-like structure and we study their spectral properties via their symbol. It turns out that the symbol:

- (a) only vanishes at 0 where it has a zero of order α ;
- (b) presents an exponential decay to zero at π for increasing p , a so-called numerical zero, that becomes faster as α approaches 1;
- (c) is bounded from below in the proximity of π by a positive function independent of α .

This translates into a mitigated conditioning in the low frequencies and into a deterioration in the high frequencies when compared to second order problems (see Reference 30). The symbol, and so the (asymptotic) spectral properties of the involved matrices, do not change if reaction and/or advection terms are added to (1).

As a side result of the symbol computation, we propose a new way of expressing both left and right fractional derivatives of a cardinal B-spline as inner products of two fractional derivatives of cardinal B-splines.

Furthermore, we provide a numerical study of the approximation behavior of polynomial B-spline collocation for an arbitrary degree p . It turns out that the approximation order for smooth solutions is $p + 2 - \alpha$ for even p , and $p + 1 - \alpha$ for odd p . This is in agreement with the approximation results known for standard (nonfractional) diffusion problems.³¹ We refer the reader to References 6,32,33 for a smoothness analysis of the solution in (weighted) Sobolev spaces.

The paper is organized as follows. Section 2 is devoted to notations, definitions, and preliminary results. In Section 3 we present a new way of writing the fractional derivative of a cardinal B-spline. In Section 4 we describe the IgA collocation approximation of the problem reported in (1), while in Sections 5 and 6 we perform a detailed spectral analysis of the resulting coefficient matrices. We validate our theoretical spectral findings with a selection of numerical experiments in Section 7 and we do a numerical study of the approximation order of the polynomial B-spline collocation method as well. We end with some concluding remarks in Section 8.

2 | PRELIMINARIES

In this section, we collect some preliminary tools on fractional derivatives, spectral analysis, and IgA discretizations. Firstly, we give two definitions of fractional derivatives (Section 2.1). Secondly, after introducing the definition of spectral distribution of general matrix-sequences, we summarize the essentials of Toeplitz sequences (Section 2.2). Finally, we recall the definition of B-splines and cardinal B-splines (Section 2.3).

2.1 | Fractional derivatives

A common definition of fractional derivatives is given by the Riemann–Liouville formula. For a given function u with absolutely continuous $(m - 1)$ th derivative on $[a, b]$, the left and right Riemann–Liouville fractional derivatives of order α are defined by

$$\begin{aligned} {}^RLD_x^\alpha u(x) &:= \frac{1}{\Gamma(m - \alpha)} \frac{d^m}{dx^m} \int_a^x (x - y)^{m-\alpha-1} u(y) dy, \\ {}^RLD_b^\alpha u(x) &:= \frac{(-1)^m}{\Gamma(m - \alpha)} \frac{d^m}{dx^m} \int_x^b (y - x)^{m-\alpha-1} u(y) dy, \end{aligned}$$

with m the integer such that $m - 1 \leq \alpha < m$ and Γ the Euler gamma function. Note that the left fractional derivative of the function u computed at x depends on all function values to the left of x , while the right fractional derivative depends on the ones to the right.

Another common definition of fractional derivative was proposed by Caputo:

$$\begin{aligned} {}^CD_x^\alpha u(x) &:= \frac{1}{\Gamma(m - \alpha)} \int_a^x (x - y)^{m-\alpha-1} u^{(m)}(y) dy, \\ {}^CD_b^\alpha u(x) &:= \frac{(-1)^m}{\Gamma(m - \alpha)} \int_x^b (y - x)^{m-\alpha-1} u^{(m)}(y) dy. \end{aligned} \tag{2}$$

Note that (2) requires the m th derivative of u to be absolutely integrable. Higher regularity of the solution is typically imposed in time rather than in space. As a consequence, the Caputo formulation is mainly used for fractional derivatives

in time, while Riemann–Liouville’s is preferred for fractional derivatives in space. The use of Caputo’s derivative provides some advantages in the treatment of boundary conditions when applying the Laplace transform method (see chapter 2.8 in Reference 34).

The Riemann–Liouville derivatives are related to the Caputo ones as follows:

$$\begin{aligned}
 {}^{RL}D_x^\alpha u(x) &= {}^C D_x^\alpha u(x) + \sum_{k=0}^{m-1} \frac{(x-a)^{k-\alpha}}{\Gamma(k-\alpha+1)} u^{(k)}(a^+), \\
 {}^{RL}D_b^\alpha u(x) &= {}^C D_b^\alpha u(x) + \sum_{k=0}^{m-1} \frac{(-1)^k (b-x)^{k-\alpha}}{\Gamma(k-\alpha+1)} u^{(k)}(b^-),
 \end{aligned}
 \tag{3}$$

and the two coincide if u satisfies homogeneous conditions, that is, $u^{(k)}(a^+) = u^{(k)}(b^-) = 0$ for $k = 0, \dots, m-1$, where $u^{(k)}(a^+)$ and $u^{(k)}(b^-)$ denote the right- and left-sided limits of $u^{(k)}(x)$ at a and b , respectively.

Remark 1. Throughout the paper, whenever we write ${}^{RL}D_x^\alpha u(\xi)$ or ${}^{RL}D_b^\alpha u(\xi)$ for a fixed ξ we mean ${}^{RL}D_x^\alpha u(x)$ or ${}^{RL}D_b^\alpha u(x)$, where $x = \xi$, respectively.

2.2 | Spectral tools

We begin with the formal definition of spectral distribution in the sense of the eigenvalues for a general matrix-sequence.

Definition 1. Let $f : G \rightarrow \mathbb{C}$ be a measurable function, defined on a measurable set $G \subset \mathbb{R}^k$ with $k \geq 1$ and Lebesgue measure $0 < \mu_k(G) < \infty$. Let $C_0(\mathbb{C})$ be the set of continuous functions with compact support over \mathbb{C} , and let A_n be a matrix of size d_n with eigenvalues $\lambda_j(A_n), j = 1, \dots, d_n$. The matrix-sequence $\{A_n\}_n$ (with $d_n < d_{n+1}$) is distributed as the pair (f, G) in the sense of the eigenvalues, denoted by

$$\{A_n\}_n \sim_\lambda (f, G),$$

if the following limit relation holds for all $F \in C_0(\mathbb{C})$:

$$\lim_{n \rightarrow \infty} \frac{1}{d_n} \sum_{j=1}^{d_n} F(\lambda_j(A_n)) = \frac{1}{\mu_k(G)} \int_G F(f(t)) \, dt. \tag{4}$$

We say that f is the (spectral) symbol of the matrix-sequence $\{A_n\}_n$.

Remark 2. Throughout the paper, when it is not of crucial importance to know what is the domain of f , we replace the notation $\{A_n\}_n \sim_\lambda (f, G)$ with $\{A_n\}_n \sim_\lambda f$.

Remark 3. When f is continuous, an informal interpretation of the limit relation (4) is that when the matrix-size is sufficiently large, the eigenvalues of A_n can be approximated by a sampling of f on a uniform equispaced grid of the domain G , possibly up to few outliers.

For a given matrix $X \in \mathbb{C}^{m \times m}$, let us denote by $\|X\|_{1,*}$ the trace norm defined by $\|X\|_{1,*} := \sum_{j=1}^m \sigma_j(X)$, where $\sigma_j(X)$ are the m singular values of X .

The following result allows us to determine the spectral distribution of a Hermitian matrix-sequence plus a correction (see Reference 35 (corollary 4.1) and also Reference 36 for an extension).

Theorem 1. Let $\{X_n\}_n$ and $\{Y_n\}_n$ be two matrix-sequences, with $X_n, Y_n \in \mathbb{C}^{d_n \times d_n}$, and assume that

- (a) X_n is Hermitian for all n and $\{X_n\}_n \sim_\lambda f$;
- (b) $\|X_n\|_2, \|Y_n\|_2 \leq C$ for all n with C a constant independent of d_n and with $\|\cdot\|_2$ the spectral norm;
- (c) $\|Y_n\|_{1,*} = o(d_n)$ as $n \rightarrow \infty$.

Then, $\{X_n + Y_n\}_n \sim_\lambda f$.

We now recall the definition of Toeplitz sequences generated by univariate functions in $L^1([-\pi, \pi])$.

Definition 2. Let $f \in L^1([-\pi, \pi])$ and let f_k be its Fourier coefficients,

$$f_k := \frac{1}{2\pi} \int_{-\pi}^{\pi} f(\theta) e^{-i(k\theta)} d\theta, \quad k \in \mathbb{Z}. \tag{5}$$

The n th Toeplitz matrix associated with f is the $n \times n$ matrix defined by

$$T_n(f) := \begin{bmatrix} f_0 & f_{-1} & \cdots & \cdots & f_{-(n-1)} \\ f_1 & \ddots & \ddots & & \vdots \\ \vdots & \ddots & \ddots & \ddots & \vdots \\ \vdots & & \ddots & \ddots & f_{-1} \\ f_{n-1} & \cdots & \cdots & f_1 & f_0 \end{bmatrix} \in \mathbb{C}^{n \times n}. \tag{6}$$

The matrix-sequence $\{T_n(f)\}_n$ is called the Toeplitz sequence generated by f .

For real-valued Toeplitz matrix-sequences, the following theorem holds (see, e.g., Reference 37).

Theorem 2. Let $f \in L^1([\pi, \pi])$ be a real-valued function. Then,

$$\{T_n(f)\}_n \sim_{\lambda} (f, [-\pi, \pi]).$$

2.3 | B-splines and cardinal B-splines

For $p \geq 0$ and $n \geq 1$, consider the following uniform open knot sequence corresponding to a uniform mesh of $[0, 1]$, consisting of n intervals:

$$\xi_1 = \cdots = \xi_{p+1} := 0 < \xi_{p+2} < \cdots < \xi_{p+n} < 1 =: \xi_{p+n+1} = \cdots = \xi_{2p+n+1},$$

where

$$\xi_{i+p+1} := \frac{i}{n}, \quad i = 0, \dots, n.$$

This knot sequence allows us to define $n + p$ B-splines of degree p .

Definition 3. The B-splines of degree p over a uniform mesh of $[0, 1]$, consisting of n intervals, are denoted by

$$N_i^p : [0, 1] \rightarrow \mathbb{R}, \quad i = 1, \dots, n + p,$$

and defined recursively as follows: for $1 \leq i \leq n + 2p$,

$$N_i^0(x) := \begin{cases} 1, & x \in [\xi_i, \xi_{i+1}), \\ 0, & \text{otherwise;} \end{cases}$$

for $1 \leq k \leq p$ and $1 \leq i \leq n + 2p - k$,

$$N_i^k(x) := \frac{x - \xi_i}{\xi_{i+k} - \xi_i} N_i^{k-1}(x) + \frac{\xi_{i+k+1} - x}{\xi_{i+k+1} - \xi_{i+1}} N_{i+1}^{k-1}(x),$$

where a fraction with zero denominator is assumed to be zero.

It is well known that the B-splines $N_i^p, i = 1, \dots, n + p$, are linearly independent and they enjoy the following list of properties (see, e.g., References 38 and 39).

- Local support:

$$\text{supp}(N_i^p) = [\xi_i, \xi_{i+p+1}], \quad i = 1, \dots, n + p; \tag{7}$$

- Smoothness:

$$N_i^p \in C^{p-1}(0, 1), \quad i = 1, \dots, n + p;$$

- Differentiation:

$$(N_i^p(x))' = p \left(\frac{N_i^{p-1}(x)}{\xi_{i+p} - \xi_i} - \frac{N_{i+1}^{p-1}(x)}{\xi_{i+p+1} - \xi_{i+1}} \right), \quad i = 1, \dots, n + p, \quad p \geq 1; \tag{8}$$

- Non-negative partition of unity:

$$N_i^p(x) \geq 0, \quad i = 1, \dots, n + p, \quad \sum_{i=1}^{n+p} N_i^p(x) = 1;$$

- Vanishing at the boundary:

$$N_i^p(0) = N_i^p(1) = 0, \quad i = 2, \dots, n + p - 1; \tag{9}$$

- Bound for the second derivatives:

$$|(N_i^p(x))''| \leq 4p(p - 1)n^2, \quad x \in (0, 1) \text{ a.e.} \tag{10}$$

We also add a property concerning fractional derivatives, which follows from (3) and (8)–(9).

- The Riemann–Liouville and the Caputo derivatives of interior B-splines coincide:

$$\begin{aligned} {}_0^{\text{RL}}D_x^\alpha N_i^p &= {}_0^{\text{C}}D_x^\alpha N_i^p, \\ {}_x^{\text{RL}}D_1^\alpha N_i^p &= {}_x^{\text{C}}D_1^\alpha N_i^p, \end{aligned} \quad i = m + 1, \dots, n + p - m.$$

From now onwards, we will denote the left and right Riemann–Liouville derivatives simply by ${}_0D_x^\alpha$ and ${}_xD_1^\alpha$. In view of the last B-spline property, these also stand for the left and right Caputo derivatives in case of interior B-splines.

The B-splines $N_i^p, i = p + 1, \dots, n$, are uniformly shifted and scaled versions of a single shape function, the so-called cardinal B-spline $\phi_p : \mathbb{R} \rightarrow \mathbb{R}$,

$$\phi_0(t) := \begin{cases} 1, & t \in [0, 1), \\ 0, & \text{otherwise,} \end{cases} \tag{12}$$

and

$$\phi_p(t) := \frac{t}{p} \phi_{p-1}(t) + \frac{p+1-t}{p} \phi_{p-1}(t-1), \quad p \geq 1. \tag{13}$$

More precisely, we have

$$N_i^p(x) = \phi_p(nx - i + p + 1), \quad i = p + 1, \dots, n,$$

and

$$(N_i^p(x))' = n\phi_p'(nx - i + p + 1), \quad i = p + 1, \dots, n.$$

The cardinal B-spline ϕ_p belongs to $C^{p-1}(\mathbb{R})$ and is supported on the interval $[0, p + 1]$. It is a symmetric function with respect to $\frac{p+1}{2}$, the midpoint of its support. The left Caputo derivative of ϕ_p has the following explicit expression (see formula (47) in Reference 25):

$${}_0D_t^\alpha \phi_p(t) = \frac{1}{\Gamma(p - \alpha + 1)} \sum_{j=0}^{p+1} (-1)^j \binom{p+1}{j} (t-j)_+^{p-\alpha}, \quad 0 \leq \alpha < p, \tag{14}$$

where $(\cdot)_+^q := (\max\{0, \cdot\})^q$ is the truncated power function of degree q . Note that the function in (14) is a fractional spline, that is, a spline with fractional degree.⁴⁰ For other common properties of cardinal B-splines, we refer the reader to Reference 39 and references therein.

3 | FRACTIONAL DERIVATIVES OF CARDINAL B-SPLINES

The aim of this section is to write the fractional derivative of a cardinal B-spline as the inner product of fractional derivatives of cardinal B-splines (see Theorem 3). This result will be used in Section 5 to derive an explicit expression of the symbol of the coefficient matrices of interest.

All the results in this section refer to fractional derivatives on the half-axes. More precisely, for a given compactly supported function u with absolutely continuous $(m - 1)$ th derivative on \mathbb{R} , we consider

$$\begin{aligned} -\infty D_x^\alpha u(x) &:= \frac{1}{\Gamma(m - \alpha)} \frac{d^m}{dx^m} \int_{-\infty}^x (x - y)^{m-\alpha-1} u(y) \, dy, \\ {}_x D_{+\infty}^\alpha u(x) &:= \frac{(-1)^m}{\Gamma(m - \alpha)} \frac{d^m}{dx^m} \int_x^{+\infty} (y - x)^{m-\alpha-1} u(y) \, dy, \end{aligned} \tag{15}$$

with m the integer such that $m - 1 \leq \alpha < m$. For functions u that are solutions of problem (1) and $m = 2$, these derivatives reduce to ${}_0 D_x^\alpha u(x)$ and ${}_x D_1^\alpha u(x)$ since the adopted boundary conditions ensure u to be identically zero on $\mathbb{R} \setminus (0, 1)$.

Let \hat{f} denote the Fourier transform of $f \in L_1(\mathbb{R}) \cap L_2(\mathbb{R})$, that is,

$$\hat{f}(\theta) := \int_{\mathbb{R}} f(x) e^{-i\theta x} \, dx.$$

We start with a lemma addressing the Fourier transform of the derivatives in (15) for cardinal B-splines.

Lemma 1. *Let ϕ_p be the cardinal B-spline as defined in (12)–(13). Then, for $0 \leq \alpha < p$ we have*

$$\widehat{-\infty D_x^\alpha \phi_p}(\theta) = (i\theta)^\alpha \left(\frac{1 - e^{-i\theta}}{i\theta} \right)^{p+1}, \tag{16}$$

and

$$\widehat{{}_x D_{+\infty}^\alpha \phi_p}(\theta) = (-i\theta)^\alpha \left(\frac{1 - e^{-i\theta}}{i\theta} \right)^{p+1}. \tag{17}$$

Proof. From Reference 34 we know that

$$\widehat{-\infty D_x^\alpha f}(\theta) = (i\theta)^\alpha \hat{f}(\theta), \quad \widehat{{}_x D_{+\infty}^\alpha f}(\theta) = (-i\theta)^\alpha \hat{f}(\theta),$$

and from References 41 and 39,

$$\widehat{\phi_p}(\theta) = \left(\frac{1 - e^{-i\theta}}{i\theta} \right)^{p+1}.$$

Combining these results immediately gives (16) and (17). ■

We are now ready for the main result of this section. In the following α_1, α_2 stand for real numbers.

Theorem 3. *Let ϕ_p be the cardinal B-spline as defined in (12)–(13). Then, for $0 \leq \alpha_1 < p_1$ and $0 \leq \alpha_2 < p_2$ we have*

$$\int_{\mathbb{R}} -\infty D_x^{\alpha_1} \phi_{p_1}(x) \, {}_x D_{+\infty}^{\alpha_2} \phi_{p_2}(x+k) \, dx = -\infty D_x^{\alpha_1+\alpha_2} \phi_{p_1+p_2+1}(p_2+1-k), \tag{18}$$

$$\int_{\mathbb{R}} {}_x D_{+\infty}^{\alpha_1} \phi_{p_1}(x) \, -\infty D_x^{\alpha_2} \phi_{p_2}(x+k) \, dx = {}_x D_{+\infty}^{\alpha_1+\alpha_2} \phi_{p_1+p_2+1}(p_2+1-k). \tag{19}$$

Proof. We first recall the Parseval identity for Fourier transforms, that is,

$$\int_{\mathbb{R}} \varphi(x) \overline{\psi(x)} \, dx = \frac{1}{2\pi} \int_{\mathbb{R}} \hat{\varphi}(\theta) \overline{\hat{\psi}(\theta)} \, d\theta, \quad \varphi, \psi \in L_2(\mathbb{R}),$$

and the translation property of the Fourier transform, that is,

$$\widehat{\psi(\cdot + k)}(\theta) = \hat{\psi}(\theta) e^{ik\theta}, \quad \psi \in L_1(\mathbb{R}), \, k \in \mathbb{R}.$$

Moreover, we recall that $(i\theta)^{\alpha_1} \overline{(-i\theta)^{\alpha_2}} = (i\theta)^{\alpha_1 + \alpha_2}$.

Starting from the above equalities, and using Lemma 1, we get

$$\begin{aligned} \int_{\mathbb{R}} {}_{-\infty}D_x^{\alpha_1} \phi_{p_1}(x) {}_xD_{+\infty}^{\alpha_2} \phi_{p_2}(x+k) \, dx &= \frac{1}{2\pi} \int_{\mathbb{R}} \widehat{{}_{-\infty}D_x^{\alpha_1} \phi_{p_1}}(\theta) \overline{\widehat{{}_xD_{+\infty}^{\alpha_2} \phi_{p_2}}(\theta)} e^{ik\theta} \, d\theta \\ &= \frac{1}{2\pi} \int_{\mathbb{R}} (i\theta)^{\alpha_1 + \alpha_2} \left(\frac{1 - e^{-i\theta}}{i\theta} \right)^{p_1+1} \left(\frac{e^{i\theta} - 1}{i\theta} \right)^{p_2+1} e^{-ik\theta} \, d\theta \\ &= \frac{1}{2\pi} \int_{\mathbb{R}} (i\theta)^{\alpha_1 + \alpha_2} \left(\frac{1 - e^{-i\theta}}{i\theta} \right)^{p_1+p_2+2} e^{i(p_2+1-k)\theta} \, d\theta. \end{aligned}$$

By taking the inverse Fourier transform of the right-hand side we arrive at (18). The proof of (19) is analogous. ■

Remark 4. Theorem 3 is a generalization of a known explicit formula for inner products of integer derivatives of cardinal B-splines (see Reference 42 and also References 39 and 43).

4 | IGA COLLOCATION DISCRETIZATION OF THE FRACTIONAL RIESZ OPERATOR

From now onwards, we assume that α is fixed in the open interval $(1, 2)$. Let \mathcal{W} be a finite dimensional vector space of sufficiently smooth functions defined on the closure of Ω and vanishing at its boundary, and let $N := \dim(\mathcal{W})$. Applying the collocation method to (1) means looking for a function $u_{\mathcal{W}} \in \mathcal{W}$ such that

$$\frac{d^\alpha u_{\mathcal{W}}(x_i)}{d|x|^\alpha} = s(x_i), \quad i = 1, \dots, N, \tag{20}$$

with $x_i \in \Omega$, the so-called collocation points. Given a basis $\{\varphi_j : j = 1, \dots, N\}$ of \mathcal{W} , problem (20) can be rewritten in matrix form as follows:

$$A_{\text{col}} \mathbf{u} = \mathbf{b}_{\text{col}},$$

with

$$A_{\text{col}} := \left[\frac{1}{2 \cos(\pi\alpha/2)} ({}_0D_x^\alpha + {}_xD_1^\alpha) \varphi_j(x_i) \right]_{i,j=1}^N, \quad \mathbf{b}_{\text{col}} := [s(x_i)]_{i=1}^N,$$

and $\mathbf{u} := [u_1, \dots, u_N]^T$ such that $u_{\mathcal{W}}(x) = \sum_{j=1}^N u_j \varphi_j(x)$. In this paper, we choose \mathcal{W} as the space of splines of degree $p \geq 2$ that vanish at the boundary, and the collocation points as the Greville abscissae. More precisely, we take

- the approximation space as the space spanned by the B-splines of degree $p \geq 2$ that are zero at the boundary (see (9)), that is,

$$\mathbb{S}_n^p := \text{span}\{N_i^p : i = 2, \dots, n + p - 1\}; \tag{21}$$

- the collocation points as the Greville abscissae corresponding to the B-splines in (21), that is,

$$\eta_i := \frac{\xi_{i+1} + \dots + \xi_{i+p}}{p}, \quad i = 2, \dots, n + p - 1.$$

Thus (20) translates into the following linear system

$$A_n^{p,\alpha} \mathbf{u}_n = \mathbf{b}_n, \tag{22}$$

where

$$A_n^{p,\alpha} := \frac{1}{2 \cos(\pi\alpha/2)} (A_n^L + A_n^R), \quad \mathbf{b}_n := [s(\eta_{i+1})]_{i=1}^{n+p-2},$$

with

$$A_n^L := \left[{}_0D_x^\alpha N_{j+1}^p(\eta_{i+1}) \right]_{i,j=1}^{n+p-2}, \quad A_n^R := \left[{}_xD_1^\alpha N_{j+1}^p(\eta_{i+1}) \right]_{i,j=1}^{n+p-2}, \tag{23}$$

and $\mathbf{u}_n := [u_1, \dots, u_{n+p-2}]^T$, the vector of the coefficients of $u_{\mathcal{V}}$ with respect to the B-spline basis functions in the space \mathbb{S}_n^p .

In order to assemble the matrices A_n^L and A_n^R , we need to compute the left and right fractional derivatives of any B-spline. By using (14), for the B-splines N_i^p corresponding to the indices $i = p + 1, \dots, n$, we have

$$\begin{aligned} {}_0D_x^\alpha N_i^p(x) &= n^\alpha {}_0D_{nx}^\alpha \phi_p(nx - i + p + 1) \\ &= \frac{n^\alpha}{\Gamma(p - \alpha + 1)} \sum_{j=0}^{p+1} (-1)^j \binom{p+1}{j} (nx - i + p + 1 - j)_+^{p-\alpha}. \end{aligned}$$

Thanks to this relation, and recalling that the Greville abscissae for $i = p + 1, \dots, n$ reduce to

$$\eta_i = \frac{i}{n} - \frac{p+1}{2n}, \quad i = p + 1, \dots, n,$$

or equivalently,

$$n\eta_i + p + 1 = i + \frac{p+1}{2}, \quad i = p + 1, \dots, n,$$

we can immediately recognize that the central part of the matrix A_n^L corresponding to the indices $p + 1, \dots, n$ has a Toeplitz structure. In other words, we have

$$A_n^L = n^\alpha (T_n^L + R_n^L),$$

where

$$T_n^L := \left[{}_0D_{nx}^\alpha \phi_p \left(\frac{p+1}{2} + i - j \right) \right]_{i,j=1}^{n+p-2},$$

and R_n^L is a matrix whose rank is bounded by $4(p - 1)$. A similar reasoning can be applied to the matrix A_n^R , and we have

$$A_n^R = n^\alpha (T_n^R + R_n^R),$$

where

$$T_n^R := \left[{}_{nx}D_n^\alpha \phi_p \left(\frac{p+1}{2} + i - j \right) \right]_{i,j=1}^{n+p-2},$$

and R_n^R is a matrix whose rank is bounded by $4(p - 1)$. As a consequence, the coefficient matrix $A_n^{p,\alpha}$ inherits the Toeplitz plus rank correction structure and can be written as follows:

$$A_n^{p,\alpha} = \frac{1}{2 \cos(\pi\alpha/2)} (A_n^L + A_n^R) = n^\alpha (T_n^{p,\alpha} + R_n^{p,\alpha}), \tag{24}$$

with

$$T_n^{p,\alpha} := \frac{1}{2 \cos(\pi\alpha/2)}(T_n^L + T_n^R), \quad R_n^{p,\alpha} := \frac{1}{2 \cos(\pi\alpha/2)}(R_n^L + R_n^R). \tag{25}$$

In Section 6 we will show that the symbol of $\{n^{-\alpha}A_n^{p,\alpha}\}_n$ coincides with the symbol of $\{T_n^{p,\alpha}\}_n$, denoted by $f^{p,\alpha}$, but first we discuss some properties of this function in the next section.

5 | PROPERTIES OF THE FUNCTION $f^{p,\alpha}$

We start with a theorem that provides an explicit expression of the generating function $f^{p,\alpha}$ of the Toeplitz matrix $T_n^{p,\alpha}$ and whose proof uses the results obtained in Section 3.

Theorem 4. *Let $\alpha \in (1, 2)$ and let $T_n^{p,\alpha}$ be defined as in (25). Then, $T_n^{p,\alpha} = T_{n+p-2}(f^{p,\alpha})$ with*

$$f^{p,\alpha}(\theta) = \sum_{l \in \mathbb{Z}} |\theta + 2l\pi|^\alpha \left(\frac{\sin(\theta/2 + l\pi)}{\theta/2 + l\pi} \right)^{p+1}. \tag{26}$$

Proof. From its construction it is clear that $T_n^{p,\alpha}$ is a Toeplitz matrix of dimension $n + p - 2$. According to the definition in (6), the entries f_k of this matrix are given by

$$f_k = \frac{1}{2 \cos(\pi\alpha/2)} \left(-_\infty D_x^\alpha \phi_p \left(\frac{p+1}{2} - k \right) + {}_x D_{+\infty}^\alpha \phi_p \left(\frac{p+1}{2} - k \right) \right).$$

We differentiate the cases of odd and even degree p . We start by proving the expression (26) of the generating function $f^{p,\alpha}$ for $p = 2q + 1$. Using Theorem 3 (and its proof) with $\alpha = \alpha_1 + \alpha_2$ and $q = p_1 = p_2$, we have

$$\begin{aligned} 2 \cos(\pi\alpha/2)f_k &= -_\infty D_x^\alpha \phi_{2q+1}(q+1-k) + {}_x D_{+\infty}^\alpha \phi_{2q+1}(q+1-k) \\ &= \frac{1}{2\pi} \int_{\mathbb{R}} [(i\theta)^\alpha + (-i\theta)^\alpha] \left(\frac{1 - e^{-i\theta}}{i\theta} \right)^{q+1} \left(\frac{e^{i\theta} - 1}{i\theta} \right)^{q+1} e^{-ik\theta} d\theta \\ &= \frac{1}{2\pi} \int_{\mathbb{R}} 2|\theta|^\alpha \cos(\pi\alpha/2) \left| \frac{1 - e^{-i\theta}}{\theta} \right|^{2q+2} e^{-ik\theta} d\theta. \end{aligned}$$

Set

$$w(\theta) := |\theta|^\alpha \left| \frac{1 - e^{-i\theta}}{\theta} \right|^{2q+2} = |\theta|^\alpha \left(\frac{\sin(\theta/2)}{\theta/2} \right)^{2q+2}.$$

Then,

$$\begin{aligned} f_k &= \frac{1}{2\pi} \int_{\mathbb{R}} w(\theta) e^{-ik\theta} d\theta = \sum_{l \in \mathbb{Z}} \frac{1}{2\pi} \int_{(2l-1)\pi}^{(2l+1)\pi} w(\theta) e^{-ik\theta} d\theta \\ &= \sum_{l \in \mathbb{Z}} \frac{1}{2\pi} \int_{-\pi}^{\pi} w(\theta + 2l\pi) e^{-ik\theta} d\theta = \frac{1}{2\pi} \int_{-\pi}^{\pi} \left[\sum_{l \in \mathbb{Z}} w(\theta + 2l\pi) \right] e^{-ik\theta} d\theta. \end{aligned}$$

The expression (26) of the generating function $f^{p,\alpha}$ follows from (5) for $p = 2q + 1$.

Now we consider even degree $p = 2q$. Using again Theorem 3 (and its proof) with $\alpha = \alpha_1 + \alpha_2$ and $q = p_1 + 1 = p_2$, we have

$$\begin{aligned} 2 \cos(\pi\alpha/2)f_k &= -_\infty D_x^\alpha \phi_{2q}(q+1-k-1/2) + {}_x D_{+\infty}^\alpha \phi_{2q}(q+1-k-1/2) \\ &= \frac{1}{2\pi} \int_{\mathbb{R}} [(i\theta)^\alpha + (-i\theta)^\alpha] \left(\frac{1 - e^{-i\theta}}{i\theta} \right)^q \left(\frac{e^{i\theta} - 1}{i\theta} \right)^{q+1} e^{-i(k+1/2)\theta} d\theta \\ &= \frac{1}{2\pi} \int_{\mathbb{R}} 2|\theta|^\alpha \cos(\pi\alpha/2) \left| \frac{1 - e^{-i\theta}}{\theta} \right|^{2q} \left(\frac{e^{i\theta/2} - e^{-i\theta/2}}{i\theta} \right) e^{-ik\theta} d\theta. \end{aligned}$$

Here,

$$w(\theta) := |\theta|^\alpha \left| \frac{1 - e^{-i\theta}}{\theta} \right|^{2q} \left(\frac{e^{i\theta/2} - e^{-i\theta/2}}{i\theta} \right) = |\theta|^\alpha \left(\frac{\sin(\theta/2)}{\theta/2} \right)^{2q+1}.$$

Following then a similar argument as in the odd degree case, we arrive at the expression (26) of the generating function $f^{p,\alpha}$ for $p = 2q$. ■

Remark 5. The proof of Theorem 4 remains valid for $\alpha \in [0, 1) \cup (1, 2]$.

Starting from (26) and applying the same line of arguments as in the proofs of lemmas 3.4 and 3.6 in Reference 30, we obtain the following results for $f^{p,\alpha}(\theta)$.

Theorem 5. Let $f^{p,\alpha}$ be as in (26) and $\theta \in [0, \pi]$. Then, $f^{p,\alpha}(\theta) = f^{p,\alpha}(-\theta)$, and for $p > \alpha$,

$$|\theta|^\alpha \left(\frac{\sin(\theta/2)}{\theta/2} \right)^{p+1} \leq f^{p,\alpha}(\theta) \leq |\theta|^\alpha \left(\frac{\sin(\theta/2)}{\theta/2} \right)^{p+1} + C_{p,\alpha} (\sin(\theta/2))^{p+1}, \tag{27}$$

where $C_{p,\alpha}$ is a constant depending on p and α . Moreover,

$$\frac{f^{p,\alpha}(\pi)}{\max_\theta f^{p,\alpha}(\theta)} \leq \frac{f^{p,\alpha}(\pi)}{f^{p,\alpha}(\pi/2)} \leq 2^{\frac{2\alpha+1-p}{2}}. \tag{28}$$

From the bounds in (27) we can immediately deduce the vanishing properties of $f^{p,\alpha}$.

Corollary 1. Let $f^{p,\alpha}$ be as in (26). Then, $f^{p,\alpha}$ is non-negative for $\theta \in [-\pi, \pi]$, and it only vanishes at $\theta = 0$ where it has a zero of order α .

Let $\tilde{f}^{p,\alpha} := f^{p,\alpha} / \max_\theta f^{p,\alpha}(\theta)$ be the normalized version of $f^{p,\alpha}$. The inequality in (28) shows that $\tilde{f}^{p,\alpha}(\theta)$ converges exponentially to zero at $\theta = \pm\pi$ for increasing p . Hence, we say that $f^{p,\alpha}$ has a numerical zero at $\pm\pi$ for large p .

Remark 6. The upper bound in (28) depends not only on p but also on α . In this view, the decay at $\pm\pi$ of $\tilde{f}^{p,\alpha}$ is expected to become faster as α approaches 1.

In the following propositions we bound $f^{p,\alpha}(\theta)$ in terms of $f^{p,0}(\theta)$ and $f^{p,2}(\theta)$ for high enough values of $|\theta|$. We recall from section 3 in Reference 30 that $f^{p,0}$ is a positive trigonometric polynomial and $f^{p,2}$ a non-negative one.

Proposition 1. For p odd, we have

$$f^{p,0}(\theta) \leq f^{p,\alpha}(\theta) \leq f^{p,2}(\theta), \quad |\theta| \in [1, \pi]. \tag{29}$$

Proof. Since

$$1 = |\theta + 2l\pi|^0 \leq |\theta + 2l\pi|^\alpha \leq |\theta + 2l\pi|^2, \quad l \in \mathbb{Z}, \quad |\theta| \geq 1,$$

and

$$\left(\frac{\sin(\theta/2 + l\pi)}{\theta/2 + l\pi} \right)^{2q+2} \geq 0, \quad l \in \mathbb{Z},$$

it is clear from the definition of $f^{p,\alpha}$ in (26) that (29) holds for $p = 2q + 1$. ■

Proposition 2. For p even and $p > \alpha$, we have

$$f^{p,0}(\theta) \leq f^{p,\alpha}(\theta), \quad |\theta| \in [a, \pi], \tag{30}$$

where

$$a := \left(\frac{\pi^4}{48} \right)^{1/\alpha}.$$

Proof. Let $p = 2q > \alpha$ and $\theta \in [-\pi, \pi]$. It is easy to check that

$$f^{p,\alpha}(\theta) = |\theta|^\alpha \left(\frac{\sin(\theta/2)}{\theta/2} \right)^{p+1} + (2 \sin(\theta/2))^{p+1} r^{p,\alpha}(\theta),$$

where

$$r^{p,\alpha}(\theta) := \sum_{k=1}^{\infty} (-1)^k \left[\frac{1}{(2k\pi + \theta)^{p+1-\alpha}} - \frac{1}{(2k\pi - \theta)^{p+1-\alpha}} \right].$$

With the same line of arguments as in the proof of lemma A.2 in Reference 30 we deduce that $r^{p,\alpha}(\theta)$ is a strictly increasing function, which implies that $r^{p,\alpha}(\pi) \geq r^{p,\alpha}(\theta) > r^{p,\alpha}(0) = 0$ for $\theta \in (0, \pi]$. Moreover, from the same lemma we know

$$r^{p,0}(\theta) \leq \left(\frac{\pi^4}{48} - 1 \right) \frac{1}{\pi^{p+1}}, \quad \theta \in [0, \pi].$$

From the above bounds we get

$$\begin{aligned} f^{p,\alpha}(\theta) - f^{p,0}(\theta) &= (|\theta|^\alpha - 1) \left(\frac{\sin(\theta/2)}{\theta/2} \right)^{p+1} + (2 \sin(\theta/2))^{p+1} (r^{p,\alpha}(\theta) - r^{p,0}(\theta)) \\ &\geq (2 \sin(\theta/2))^{p+1} \left[\frac{|\theta|^\alpha - 1}{\theta^{p+1}} - \left(\frac{\pi^4}{48} - 1 \right) \frac{1}{\pi^{p+1}} \right] \\ &\geq \left(\frac{2 \sin(\theta/2)}{\pi} \right)^{p+1} \left[|\theta|^\alpha - 1 - \left(\frac{\pi^4}{48} - 1 \right) \right], \end{aligned}$$

for $\theta \in [1, \pi]$. Hence,

$$f^{p,\alpha}(\theta) - f^{p,0}(\theta) \geq 0, \quad \theta \geq \left(\frac{\pi^4}{48} \right)^{1/\alpha},$$

and the symmetry property of $f^{p,\alpha}$ (see Theorem 5) concludes the proof. ■

In our final proposition we explicitly state that $f^{p,\alpha}$ is the symbol of the matrix-sequence $\{T_n^{p,\alpha}\}_n$.

Proposition 3. *The Toeplitz matrix $T_n^{p,\alpha}$ defined in (25) is symmetric and*

$$\{T_n^{p,\alpha}\}_n \sim_\lambda (f^{p,\alpha}, [-\pi, \pi]), \tag{31}$$

where $f^{p,\alpha}$ is given in (26).

Proof. From Theorem 5 we know that $f^{p,\alpha}$ is an even real-valued function, so the matrix $T_n^{p,\alpha} = T_{n+p-2}(f^{p,\alpha})$ is symmetric. The spectral distribution of $\{T_n^{p,\alpha}\}_n = \{T_{n+p-2}(f^{p,\alpha})\}_n$ follows from Theorem 2. ■

We end this section by summarizing all the discussed properties of the symbol $f^{p,\alpha}$ and highlighting what is their role in the design of an ad hoc solver for a linear system associated with $T_n^{p,\alpha}$ (see Remark 7). We have shown that $f^{p,\alpha}$ is equipped with the following three properties:

- (a) it vanishes at 0 with order α (Corollary 1);
- (b) it presents an exponential decay to zero at π for increasing p that becomes faster as α approaches 1 (Theorem 5 and Remark 6);
- (c) it is bounded from below in the proximity of π by $f^{p,0}$ (Propositions 1 and 2).

Properties (a)–(b) give us a clear picture of what are the conditioning peculiarities of the matrix $T_n^{p,\alpha}$. Specifically, they say that $T_n^{p,\alpha}$ is poorly conditioned both in the low frequencies (with a conditioning that grows as n^α) and in the

high frequencies (with a deterioration that is driven by both p and α). Moreover, property (c) “isolates” the source of ill-conditioning in the high frequencies induced by p , meaning the symbol behaves like $f^{p,0}$ in the proximity of π , with $f^{p,0}$ a positive function well-separated from zero.

Remark 7. Based on what has been done in References 11,12,17,18, all this knowledge can be used for the design of an ad hoc solver for a linear system associated with $T_n^{p,\alpha}$. For instance, from (a) we can infer that a multigrid method with a standard choice of both prolongator and restrictor is able to cope with the standard ill-conditioning in the low frequency subspace, while from (c) we get hints on how to define a smoother that works in the subspace of high frequencies where there exists the ill-conditioning induced by p .

6 | SPECTRAL SYMBOL OF $\{n^{-\alpha}A_n^{p,\alpha}\}_n$

This section is devoted to the computation of the symbol of the matrix-sequence $\{n^{-\alpha}A_n^{p,\alpha}\}_n$. As we have already anticipated, it turns out that the symbol of $\{n^{-\alpha}A_n^{p,\alpha}\}_n$ coincides with the symbol of the Toeplitz part $\{T_n^{p,\alpha}\}_n$. The spectral distribution of $\{n^{-\alpha}A_n^{p,\alpha}\}_n$ is given in Theorem 6. Its proof uses Theorem 1 and needs several preliminary results.

For a given matrix $X := [x_{ij}]_{i,j=1}^m \in \mathbb{C}^{m \times m}$, we denote by $\|X\|_1 := \max_{j=1, \dots, m} \sum_{i=1}^m |x_{ij}|$ and $\|X\|_\infty := \max_{i=1, \dots, m} \sum_{j=1}^m |x_{ij}|$, the induced 1- and infinity-norm, respectively.

Lemma 2. Let A_n^L be defined as in (23). For $i, j = 2, \dots, n + p - 1$ we have

$$|(A_n^L)_{i-1,j-1}| \leq \begin{cases} 0, & \eta_i \leq \xi_j, \\ c_{p,\alpha}^L n^\alpha, & \xi_j < \eta_i \leq \xi_{j+p+1} + \frac{1}{n}, \\ c_{p,\alpha}^L (\eta_i - \xi_{j+p+1})^{-\alpha}, & \xi_{j+p+1} + \frac{1}{n} < \eta_i, \end{cases} \quad (32)$$

where $c_{p,\alpha}^L$ is a constant depending on p and α .

Proof. From the properties of fractional derivatives (2)–(3) and the B-spline properties (7)–(11) it follows that for $j = 2$,

$$(A_n^L)_{i-1,1} = \frac{1}{\Gamma(2-\alpha)} \int_0^{\min(\eta_i, \xi_{p+3})} (\eta_i - y)^{1-\alpha} (N_2^p)''(y) dy + \frac{pn}{\Gamma(2-\alpha)} (\eta_i)^{1-\alpha}, \quad (33)$$

and for $j = 3, \dots, n + p - 1$,

$$(A_n^L)_{i-1,j-1} = \begin{cases} 0, & \eta_i \leq \xi_j, \\ \frac{1}{\Gamma(2-\alpha)} \int_{\xi_j}^{\min(\eta_i, \xi_{j+p+1})} (\eta_i - y)^{1-\alpha} (N_j^p)''(y) dy, & \text{otherwise.} \end{cases} \quad (34)$$

We remark that $\eta_i \in (0, 1)$, $\eta_i < \eta_{i+1}$, and $\xi_{j+p+1} - \xi_j \leq \frac{p+1}{n}$. In the following, we address the three different cases in (32) separately.

If $\eta_i \leq \xi_j$, then it is clear that $(A_n^L)_{i-1,j-1} = 0$ for $j = 3, \dots, n + p - 1$. Note that $j = 2$ is not involved in this case for any i because $\xi_2 = 0 < \eta_i$.

If $\xi_j < \eta_i \leq \xi_{j+p+1} + \frac{1}{n}$, then

$$(\eta_i - y) \leq \frac{p+2}{n}, \quad y \in [\xi_j, \min(\eta_i, \xi_{j+p+1})].$$

Using (10), from (34) we get for $j = 3, \dots, n + p - 1$,

$$\begin{aligned} |(A_n^L)_{i-1,j-1}| &\leq \frac{4p(p-1)n^2}{\Gamma(2-\alpha)} \int_{\xi_j}^{\min(\eta_i, \xi_{j+p+1})} (\eta_i - y)^{1-\alpha} dy \\ &\leq \frac{4p(p-1)n^2}{\Gamma(3-\alpha)} \left(\frac{p+2}{n}\right)^{2-\alpha}. \end{aligned}$$

When $j = 2$ we have $\xi_2 = 0$ and $\frac{1}{pn} = \eta_2 \leq \eta_i \leq \xi_{p+3} + \frac{1}{n} \leq \frac{3}{n}$. Then, we find in a similar way that for $j = 2$,

$$|(A_n^L)_{i-1,1}| \leq \frac{4p(p-1)n^2}{\Gamma(3-\alpha)} \left(\frac{3}{n}\right)^{2-\alpha} + \frac{pn}{\Gamma(2-\alpha)} \left(\frac{1}{pn}\right)^{1-\alpha}.$$

We now look at the case $\xi_{j+p+1} + \frac{1}{n} < \eta_i$. This case can only happen for $2 \leq j < n$ because when $j \geq n$ we have $\xi_{j+p+1} = 1 > \eta_i$. Given $y \in [\xi_j, \xi_{j+p+1}]$, we consider the Taylor expansion of $(\eta_i - y)^{1-\alpha}$ at ξ_j , producing

$$(\eta_i - y)^{1-\alpha} = (\eta_i - \xi_j)^{1-\alpha} - (1-\alpha)(\eta_i - \omega_{i,j}(y))^{-\alpha}(y - \xi_j), \tag{35}$$

for some $\omega_{i,j}(y) \in (\xi_j, \xi_{j+p+1})$. Substituting (35) in (34) results in

$$\begin{aligned} |(A_n^L)_{i-1,j-1}| &\leq \frac{1}{\Gamma(2-\alpha)} \left| (\eta_i - \xi_j)^{1-\alpha} \int_{\xi_j}^{\xi_{j+p+1}} (N_j^p)''(y) dy \right| \\ &\quad + \frac{\alpha-1}{\Gamma(2-\alpha)} \int_{\xi_j}^{\xi_{j+p+1}} (\eta_i - \omega_{i,j}(y))^{-\alpha} (y - \xi_j) |(N_j^p)''(y)| dy. \end{aligned}$$

Observe that $(N_j^p)'(\xi_j) = (N_j^p)'(\xi_{j+p+1}) = 0$ for $3 \leq j \leq n+p-2$, and $(\eta_i - \omega_{i,j}(y)) > (\eta_i - \xi_{j+p+1})$. Then, recalling the bound in (10), we obtain for $j = 3, \dots, n-1$,

$$\begin{aligned} |(A_n^L)_{i-1,j-1}| &\leq \frac{1}{\Gamma(2-\alpha)} \left| (\eta_i - \xi_j)^{1-\alpha} ((N_j^p)'(\xi_{j+p+1}) - (N_j^p)'(\xi_j)) \right| \\ &\quad + \frac{\alpha-1}{\Gamma(2-\alpha)} 4p(p-1)n^2 \int_{\xi_j}^{\xi_{j+p+1}} (y - \xi_j) dy (\eta_i - \xi_{j+p+1})^{-\alpha} \\ &\leq \frac{\alpha-1}{\Gamma(2-\alpha)} 2p(p-1)n^2 \left(\frac{p+1}{n}\right)^2 (\eta_i - \xi_{j+p+1})^{-\alpha}. \end{aligned}$$

Substituting (35) in (33) and observing that $(N_2^p)'(0) = np$, $(N_2^p)'(\xi_{p+3}) = 0$, we find with a similar argument that for $j = 2$,

$$\begin{aligned} |(A_n^L)_{i-1,1}| &\leq \frac{1}{\Gamma(2-\alpha)} \left| (\eta_i)^{1-\alpha} ((N_2^p)'(\xi_{p+3}) - (N_2^p)'(0)) + np(\eta_i)^{1-\alpha} \right| \\ &\quad + \frac{\alpha-1}{\Gamma(2-\alpha)} 4p(p-1)n^2 \int_0^{\xi_{p+3}} y dy (\eta_i - \xi_{p+3})^{-\alpha} \\ &\leq \frac{\alpha-1}{\Gamma(2-\alpha)} 2p(p-1)n^2 \left(\frac{2}{n}\right)^2 (\eta_i - \xi_{p+3})^{-\alpha}. \end{aligned}$$

This concludes the proof. ■

Lemma 3. Let A_n^L be defined as in (23). We have

$$\|n^{-\alpha} A_n^L\|_q \leq C_{p,\alpha}^L, \quad q \in \{1, 2, \infty\},$$

where $C_{p,\alpha}^L$ is a constant depending on p and α .

Proof. We first consider the infinity-norm

$$\|n^{-\alpha} A_n^L\|_\infty = n^{-\alpha} \max_{i=2, \dots, n+p-1} \sum_{j=2}^{n+p-1} |(A_n^L)_{i-1,j-1}|.$$

The entries $|(A_n^L)_{i-1,j-1}|$, $i, j = 2, \dots, n+p-1$, can be bounded thanks to the results of Lemma 2. We observe that for any fixed i ,

- the number of indices in $\{j : \xi_j < \eta_i \leq \xi_{j+p+1} + \frac{1}{n}\}$ is bounded by $p + 2$;
- for $j = n, \dots, n + p - 1$ we have $\xi_{j+p+1} = 1$, thus either $\eta_i \leq \xi_j$ or $\xi_j < \eta_i \leq \xi_{j+p+1} + \frac{1}{n}$;
- if $\eta_i > \xi_{j+p+1} + \frac{1}{n}$, then $2 \leq j \leq n - 1$ and

$$\eta_i - \xi_{j+p+1} = \eta_i - \frac{j}{n} \geq \frac{\ell_{ij}}{n},$$

where $\ell_{ij} := \lfloor n\eta_i - j \rfloor$. Note that $\ell_{ij} \geq 1$ and $\ell_{ij} = \ell_{i,j+1} + 1$, so

$$\sum_{j: \eta_i > \xi_{j+p+1} + \frac{1}{n}} (\ell_{ij})^{-\alpha} \leq \sum_{\ell=1}^{\infty} \ell^{-\alpha} = \zeta(\alpha),$$

with $\zeta(\alpha)$ the Riemann zeta function evaluated at α . The series $\sum_{\ell=1}^{\infty} \ell^{-\alpha}$ is convergent for $\alpha \in (1, 2)$.

As a consequence, taking into account Lemma 2, for any fixed i we have

$$\begin{aligned} n^{-\alpha} \sum_{j=2}^{n+p-1} |(A_n^L)_{i-1,j-1}| &\leq n^{-\alpha} \left[\sum_{j: \xi_j < \eta_i \leq \xi_{j+p+1} + \frac{1}{n}} |(A_n^L)_{i-1,j-1}| + \sum_{j: \eta_i > \xi_{j+p+1} + \frac{1}{n}} |(A_n^L)_{i-1,j-1}| \right] \\ &\leq n^{-\alpha} c_{p,\alpha}^L \left[(p+2)n^\alpha + \sum_{j: \eta_i > \xi_{j+p+1} + \frac{1}{n}} \left(\frac{\ell_{ij}}{n}\right)^{-\alpha} \right] \\ &\leq c_{p,\alpha}^L [p+2 + \zeta(\alpha)]. \end{aligned}$$

The bound for the 1-norm

$$\|n^{-\alpha} A_n^L\|_1 = n^{-\alpha} \max_{j=2, \dots, n+p-1} \sum_{i=2}^{n+p-1} |(A_n^L)_{i-1,j-1}|$$

can be shown with a similar line of arguments, by observing that for any fixed j ,

- the number of indices in $\{i : \xi_j < \eta_i \leq \xi_{j+p+1} + \frac{1}{n}\}$ is bounded by $2p$;
- if $\eta_i > \xi_{j+p+1} + \frac{1}{n}$, then

$$\eta_i - \xi_{j+p+1} \geq \frac{\ell_{ij}}{n},$$

where $\ell_{ij} := \lfloor n(\eta_i - \xi_{j+p+1}) \rfloor$. Note that $\ell_{ij} \geq 1$ for all i and $\ell_{i+1,j} = \ell_{ij} + 1$ for $p+1 \leq i \leq n-1$, so

$$\sum_{i: \eta_i > \xi_{j+p+1} + \frac{1}{n}} (\ell_{ij})^{-\alpha} \leq 2(p-1) + \sum_{\ell=1}^{\infty} \ell^{-\alpha} = 2(p-1) + \zeta(\alpha).$$

Finally, the bound for the spectral norm follows from the inequality

$$\|n^{-\alpha} A_n^L\|_2 \leq \sqrt{\|n^{-\alpha} A_n^L\|_\infty \|n^{-\alpha} A_n^L\|_1}$$

and the above results for the infinity-norm and 1-norm. ■

A similar reasoning to the one adopted in the previous lemmas brings us to the following result.

Lemma 4. Let A_n^R be defined as in (23). We have

$$\|n^{-\alpha}A_n^R\|_q \leq C_{p,\alpha}^R, \quad q \in \{1, 2, \infty\},$$

where $C_{p,\alpha}^R$ is a constant depending on p and α .

In the next lemma we provide bounds for some norms of the matrix $R_n^{p,\alpha}$.

Lemma 5. Let $R_n^{p,\alpha}$ be defined as in (25). We have

$$\|R_n^{p,\alpha}\|_2, \|R_n^{p,\alpha}\|_{1,*} \leq \tilde{C}_{p,\alpha},$$

where $\tilde{C}_{p,\alpha}$ is a constant depending on p and α .

Proof. The relation in (24) implies

$$\|R_n^{p,\alpha}\|_2 = \|n^{-\alpha}A_n^{p,\alpha} - T_n^{p,\alpha}\|_2 \leq \|n^{-\alpha}A_n^{p,\alpha}\|_2 + \|T_n^{p,\alpha}\|_2,$$

and we recall from Section 5 that

$$\|T_n^{p,\alpha}\|_2 = \|T_{n+p-2}(f^{p,\alpha})\|_2 \leq \|f^{p,\alpha}\|_\infty < +\infty.$$

Then, by Lemmas 3–4 and (24), we arrive at

$$\|R_n^{p,\alpha}\|_2 \leq \frac{1}{2 \cos(\pi\alpha/2)} (C_{p,\alpha}^L + C_{p,\alpha}^R) + \|f^{p,\alpha}\|_\infty.$$

In addition, $\|R_n^{p,\alpha}\|_{1,*} \leq \text{rank}(R_n^{p,\alpha})\|R_n^{p,\alpha}\|_2$ and $\text{rank}(R_n^{p,\alpha}) \leq 4(p-1)$. This completes the proof. ■

We are now in a position to discuss the spectral distribution of $\{n^{-\alpha}A_n^{p,\alpha}\}_n$.

Theorem 6. Given $\{n^{-\alpha}A_n^{p,\alpha}\}_n$ with $A_n^{p,\alpha}$ as in (24), we have

$$\{n^{-\alpha}A_n^{p,\alpha}\}_n \sim_\lambda (f^{p,\alpha}, [-\pi, \pi]), \quad (36)$$

where $f^{p,\alpha}$ is given in (26).

Proof. We prove this result by applying Theorem 1 with $X_n = T_n^{p,\alpha}$ and $Y_n = R_n^{p,\alpha}$. We first note that, because of Proposition 3, condition (a) of Theorem 1 is satisfied. The other conditions hold by Lemmas 3–4 with $q = 2$ and by Lemma 5. ■

Remark 8. Thanks to Theorem 6, the matrices $n^{-\alpha}A_n^{p,\alpha}$ and $T_n^{p,\alpha}$ are asymptotically spectrally equivalent, possibly up to few outliers. As a consequence, the arguments given in Remark 7 apply unchanged when the aim is solving a linear system whose coefficient matrix is $n^{-\alpha}A_n^{p,\alpha}$ instead of $T_n^{p,\alpha}$.

Remark 9. Let $A_n^{p,\alpha,\gamma,\rho}$ be the coefficient matrix corresponding to the B-spline collocation discretization of the advection-diffusion-reaction problem

$$\begin{cases} \frac{d^\alpha u(x)}{d|x|^\alpha} + \gamma u'(x) + \rho u(x) = s(x), & x \in \Omega, \\ u(x) = 0, & x \in \mathbb{R} \setminus \Omega, \end{cases}$$

with $\rho > 0$ and $\gamma \in \mathbb{R}$. From Theorem 6, in combination with Theorem 1 and lemma 4.1 in Reference 30, we immediately deduce that

$$\{n^{-\alpha}A_n^{p,\alpha,\gamma,\rho}\}_n \sim_\lambda (f^{p,\alpha}, [-\pi, \pi]).$$

7 | NUMERICAL EXPERIMENTS

In the following, we verify the spectral results obtained in Sections 5 and 6 through several numerical experiments. We also provide a numerical study of the approximation behavior of the proposed polynomial B-spline collocation method for an arbitrary degree p .

Let us start by illustrating that

- the symbol $f^{p,\alpha}$ only vanishes at 0, where it has a zero of order α , and it presents an exponential decay to zero at π for increasing p ;
- the symbol $f^{p,\alpha}$ satisfies the bounds in (29) for odd p , and the bound in (30) for even p ;
- relations (31) and (36) hold.

Note that it suffices to consider the interval $[0, \pi]$ due to the symmetry of $f^{p,\alpha}$; see Theorem 5.

Figure 1 shows that, independently of p , the normalized symbol $\tilde{f}^{p,\alpha} := f^{p,\alpha} / \max_{\theta} f^{p,\alpha}(\theta)$ only vanishes at 0 and the order of such zero increases up to 2 as α tends to 2. On the other hand, it presents a decay at π as p increases. We observe that such decay becomes faster when α decreases to 1, in accordance with Remark 6.

In Figure 2 we show that, varying $\alpha \in \{1.2, 1.3, 1.5, 1.8\}$, the bounds in (29) hold for $p = 3$, and the one in (30) holds for $p = 4$. Observe that, despite the fact that relation (30) is only theoretically proven to be true for all $\theta \in [a, \pi]$, $a = \left(\frac{\pi^4}{48}\right)^{1/\alpha} > 1$, it actually holds for all $\theta \in [1, \pi]$.

In order to numerically verify that relations (31) and (36) hold, for fixed n, p , we define the following equispaced grid on $[0, \pi]$:

$$\Gamma := \left\{ \theta_k := \frac{k\pi}{n+p-2} : k = 1, \dots, n+p-2 \right\}.$$

Then, we compare the sampling of $f^{p,\alpha}$ on Γ with the eigenvalues of both $T_n^{p,\alpha}$ and $n^{-\alpha}A_n^{p,\alpha}$. Both eigenvalues and sampling values have been ordered in ascending way. In all the numerical experiments, the entries of the coefficient matrix

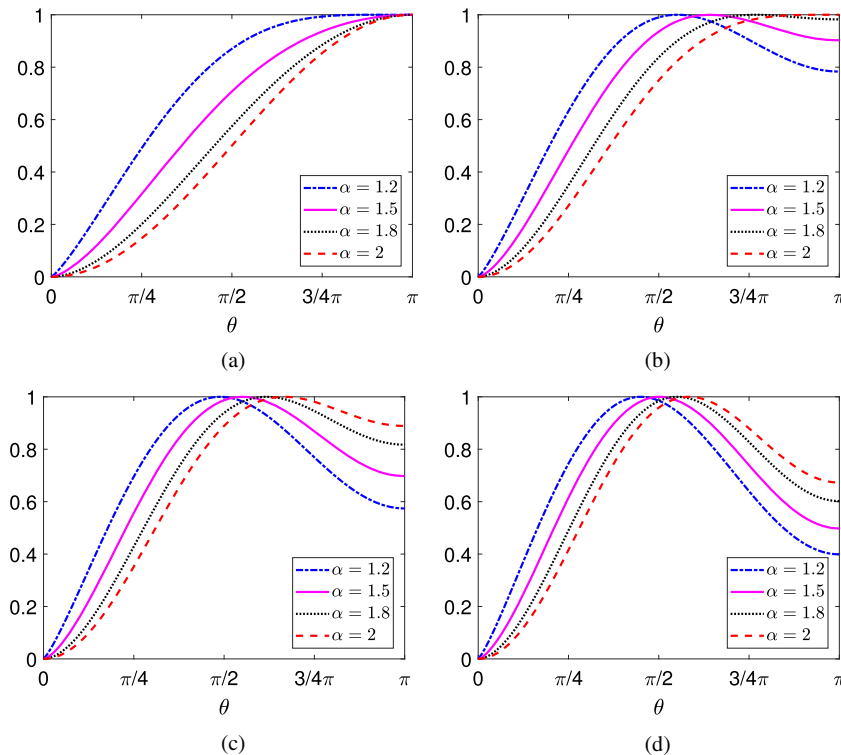


FIGURE 1 (a–d) Plot of $\tilde{f}^{p,\alpha} := f^{p,\alpha} / \max_{\theta} f^{p,\alpha}(\theta)$ for $p = 3, 4, 5, 6$. In all cases $\alpha \in \{1.2, 1.5, 1.8, 2\}$

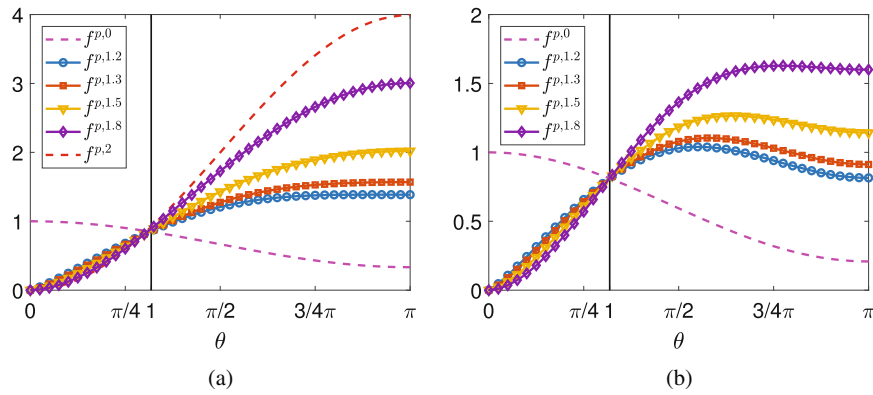


FIGURE 2 (a) Check of the bound in (29) which is valid for odd p ($p = 3$), and (b) check of the bound in (30) which is valid for even p ($p = 4$). In both cases $\alpha \in \{1.2, 1.3, 1.5, 1.8\}$

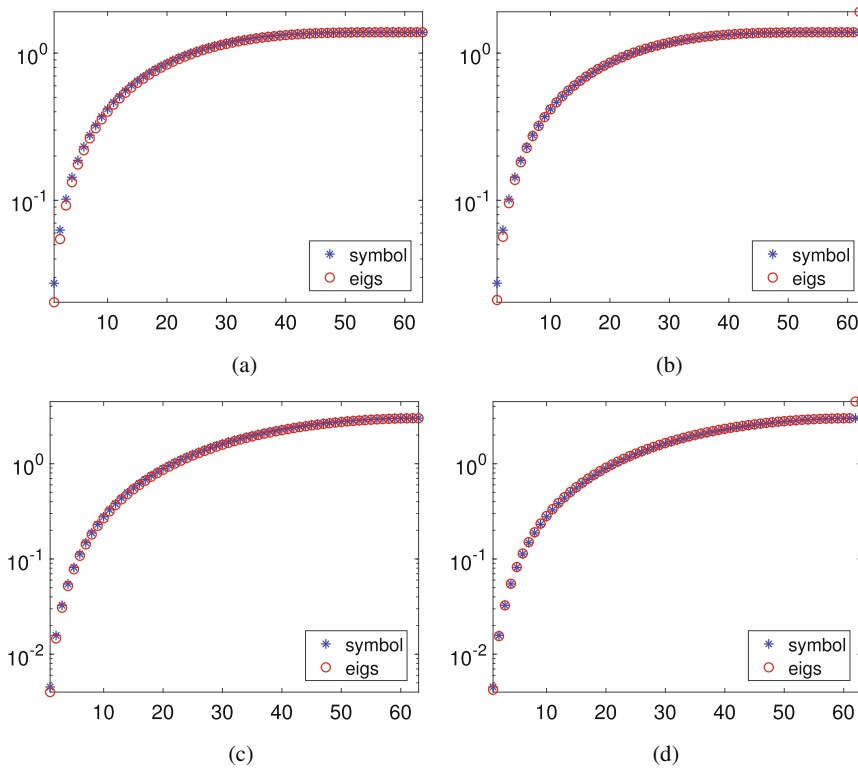


FIGURE 3 Comparison of the eigenvalues of (a,c) $T_n^{p,\alpha}$ and (b,d) $n^{-\alpha} A_n^{p,\alpha}$ (o) with a uniform sampling of $f^{p,\alpha}$ on Γ (*), ordered in ascending way, for (a,b) $\alpha = 1.2$ and (c,d) $\alpha = 1.8$. In all cases $n = 63, p = 3$

$A_n^{p,\alpha}$ have been computed using the Gauss–Jacobi-type quadrature rules introduced in Reference 44. In Figure 3 we fix $p = 3, n = 63$ and vary $\alpha \in \{1.2, 1.8\}$. For both $T_n^{p,\alpha}$ and $n^{-\alpha} A_n^{p,\alpha}$ we experience a very good matching, which is in accordance with Proposition 3 and Theorem 6. However, we observe that in the case of $n^{-\alpha} A_n^{p,\alpha}$ there are few large eigenvalues that do not behave like the symbol; these are outliers. Their number seems to depend only on p and increases in the same way as it has been observed for similar discretizations for integer-order PDEs (see, e.g., Reference 31). As a further confirmation of Proposition 3 and Theorem 6, we obtained similar results also for $p = 4, n = 62$, and $\alpha \in \{1.2, 1.8\}$; see Figure 4.

We end this section by checking how the approximation order of the considered polynomial B-spline collocation method behaves with respect to p for smooth solutions of problem (1). More precisely, in Tables 1–2 we fix the source function $s(x)$ such that the exact solution of (1) is given by

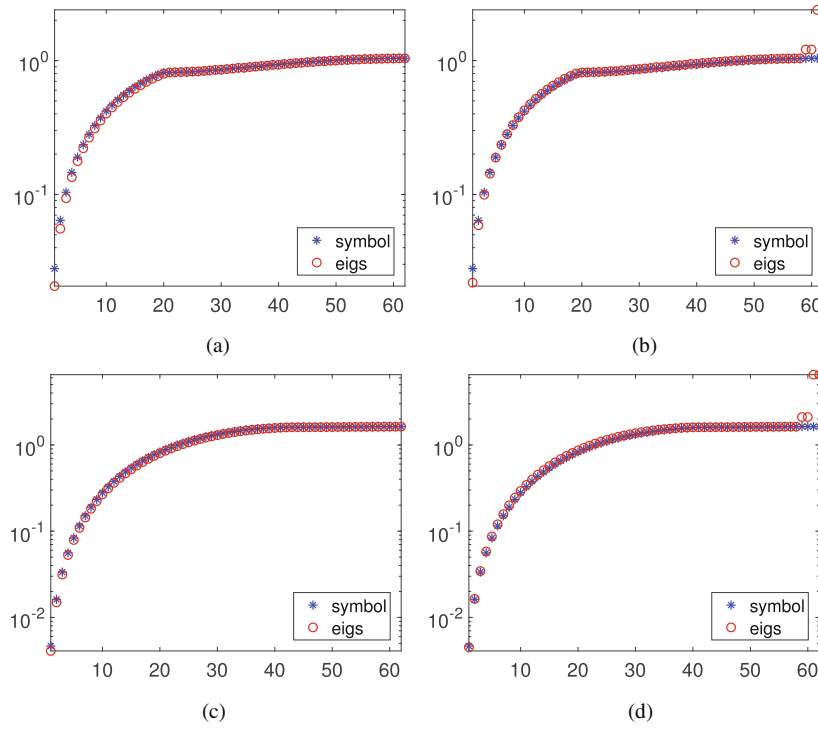


FIGURE 4 Comparison of the eigenvalues of (a,c) $T_n^{p,\alpha}$ and (b,d) $n^{-\alpha}A_n^{p,\alpha}$ (o) with a uniform sampling of $f^{p,\alpha}$ on Γ (*), ordered in ascending way, for (a,b) $\alpha = 1.2$ and (c,d) $\alpha = 1.8$. In all cases $n = 62, p = 4$

TABLE 1 Errors and convergence orders of the proposed B-spline collocation method for problem (1) when $u(x) = x^3(1 - x)^3$

α	n	$p = 2$		$p = 3$		$p = 4$		$p = 5$	
		Error	Order	Error	Order	Error	Order	Error	Order
1.2	4	1.3146e-03		1.1197e-03		2.6802e-04		4.8556e-05	
	8	1.5675e-04	3.07	9.8810e-05	3.50	1.0317e-05	4.70	3.4230e-06	3.83
	16	2.4941e-05	2.65	1.5622e-05	2.66	4.1887e-07	4.62	1.3853e-07	4.63
	32	3.5227e-06	2.82	2.4433e-06	2.68	1.6226e-08	4.69	5.1403e-09	4.75
	64	5.0507e-07	2.80	3.6711e-07	2.73	5.9986e-10	4.76	2.1670e-10	4.57
	128	7.2190e-08	2.81	5.3421e-08	2.78	5.9102e-11	3.34	7.0806e-09	-
	256	1.0343e-08	2.80	7.7127e-09	2.79	3.3823e-09	-	2.1054e-07	-
			≈ 2.8		≈ 2.8		≈ 4.8		≈ 4.8
1.5	4	1.6170e-03		1.8701e-03		3.4358e-04		8.0567e-05	
	8	1.7117e-04	3.24	2.0365e-04	3.20	1.9552e-05	4.14	7.4745e-06	3.43
	16	3.1719e-05	2.43	2.8530e-05	2.84	1.0245e-06	4.25	3.7577e-07	4.31
	32	5.8828e-06	2.43	5.7869e-06	2.30	4.9498e-08	4.37	1.7183e-08	4.45
	64	1.0458e-06	2.49	1.0661e-06	2.44	2.2995e-09	4.43	8.0703e-10	4.41
	128	1.8532e-07	2.50	1.9080e-07	2.48	8.5791e-11	4.74	2.0718e-09	-
	256	3.2838e-08	2.50	3.3858e-08	2.49	9.2926e-10	-	4.5542e-08	-
			≈ 2.5		≈ 2.5		≈ 4.5		≈ 4.5
1.8	4	1.9908e-03		3.1774e-03		4.3396e-04		1.3425e-04	
	8	2.5091e-04	2.99	4.4181e-04	2.85	3.6073e-05	3.59	1.5905e-05	3.08
	16	4.2953e-05	2.55	6.8611e-05	2.69	2.4045e-06	3.91	9.8386e-07	4.01
	32	9.3400e-06	2.20	1.3336e-05	2.36	1.4401e-07	4.06	5.5249e-08	4.15
	64	2.0702e-06	2.17	3.0292e-06	2.14	8.2251e-09	4.13	3.0499e-09	4.18
	128	4.5230e-07	2.19	6.6739e-07	2.18	4.7779e-10	4.11	1.4620e-09	-
	256	9.8595e-08	2.20	1.4568e-07	2.20	1.7086e-09	-	1.0996e-07	-
			≈ 2.2		≈ 2.2		≈ 4.2		≈ 4.2

TABLE 2 Errors and convergence orders of the proposed B-spline collocation method for problem (1) when $u(x) = \sin(\pi x^2)$

α	n	$p = 2$		$p = 3$		$p = 4$		$p = 5$	
		Error	Order	Error	Order	Error	Order	Error	Order
1.2	4	4.0099e-02		1.5948e-02		6.1393e-03		1.9341e-03	
	8	8.4523e-03	2.25	4.6043e-03	1.79	2.5317e-04	4.60	1.0271e-04	4.23
	16	1.1497e-03	2.88	7.8372e-04	2.55	7.9503e-06	4.99	2.5175e-06	5.35
	32	1.6423e-04	2.81	1.1786e-04	2.73	2.5619e-07	4.96	7.1641e-08	5.14
	64	2.3468e-05	2.81	1.7096e-05	2.79	9.5594e-09	4.74	1.0289e-08	2.80
	128	3.3396e-06	2.81	2.4609e-06	2.80	8.2740e-09	-	1.2761e-06	-
	256	4.7709e-07	2.81	3.5206e-07	2.81	1.6119e-07	-	1.9015e-05	-
			≈ 2.8		≈ 2.8		≈ 4.8		≈ 4.8
1.5	4	4.2457e-02		2.4735e-02		7.7604e-03		2.6753e-03	
	8	1.0378e-02	2.03	7.9809e-03	1.63	4.3612e-04	4.15	1.9027e-04	3.81
	16	1.7932e-03	2.53	1.7304e-03	2.21	1.7374e-05	4.65	6.3744e-06	4.90
	32	3.1466e-04	2.51	3.1905e-04	2.44	7.0999e-07	4.61	2.2599e-07	4.82
	64	5.5887e-05	2.49	5.7202e-05	2.48	2.9859e-08	4.57	7.5065e-09	4.91
	128	9.8690e-06	2.50	1.0148e-05	2.49	5.0068e-09	2.58	5.3934e-07	-
	256	1.7449e-06	2.50	1.7943e-06	2.50	1.2097e-07	-	1.3493e-06	-
			≈ 2.5		≈ 2.5		≈ 4.5		≈ 4.5
1.8	4	4.2801e-02		3.8129e-02		9.6792e-03		3.8393e-03	
	8	1.2259e-02	1.80	1.4094e-02	1.44	7.5244e-04	3.69	3.6381e-04	3.40
	16	2.7540e-03	2.15	3.8466e-03	1.87	3.9382e-05	4.26	1.6023e-05	4.50
	32	6.0215e-04	2.19	8.8181e-04	2.13	2.0021e-06	4.30	7.1827e-07	4.48
	64	1.3172e-04	2.19	1.9414e-04	2.18	1.0435e-07	4.26	3.2796e-08	4.45
	128	2.8698e-05	2.20	4.2383e-05	2.20	2.5013e-09	5.38	1.8390e-07	-
	256	6.2494e-06	2.20	9.2301e-06	2.20	6.3463e-08	-	2.1447e-05	-
			≈ 2.2		≈ 2.2		≈ 4.2		≈ 4.2

- $u(x) = x^3(1-x)^3$, and
- $u(x) = \sin(\pi x^2)$,

respectively. Then, by doubling n repeatedly, we show the infinity-norm of the corresponding errors and the convergence orders for varying p and α . The infinity-norm of the error is computed by taking the maximum value of the error sampled in 1024 points uniformly distributed over $[0, 1]$. In the case of standard (nonfractional) diffusion problems, we know that the approximation order for smooth solutions is p for even p , and $p - 1$ for odd p ; see Reference 31. In the fractional case, we observe a dependency of the approximation order on α that seems to vary as $p + 2 - \alpha$ for even p , and as $p + 1 - \alpha$ for odd p . We also observe a stagnation in the convergence for $p = 4, 5$; this is due to numerical issues in the difficult computation of the entries of the matrix $A_n^{p,\alpha}$ and the right-hand side \mathbf{b}_n in (22).

8 | CONCLUSION AND FUTURE PERSPECTIVE

We focused on a fractional differential equation in Riesz form discretized by a polynomial B-spline collocation method and we showed that, for an arbitrary degree p , the resulting coefficient matrices possess a Toeplitz-like structure. We computed and analyzed the corresponding spectral symbol. In particular, we proved that the symbol vanishes at 0 with

order α , the fractional derivative order that ranges from 1 to 2, and it presents an exponential decay to zero at π for increasing p that becomes faster as α approaches 1. This translates into a mitigated conditioning in the low frequencies and into a deterioration in the high frequencies when compared to second order problems. Moreover, we showed that the behavior of the symbol at π is well captured by the symbol corresponding to $\alpha = 0$, which is a positive trigonometric polynomial.

As a side result of the symbol computation, we ended up with a new way to express the central entries of the coefficient matrix as inner products of two fractional derivatives of cardinal B-splines.

In addition, we performed a numerical study of the approximation behavior of polynomial B-spline collocation. This study suggests that the approximation order for smooth solutions in the fractional case is $p + 2 - \alpha$ for even p , and $p + 1 - \alpha$ for odd p , which is in line with approximation results known for standard (nonfractional) diffusion problems.³¹ For large p and fine meshes, however, numerical issues were observed and require further examination.

The investigation presented here is intended as a first step towards the use of collocation methods based on high-order polynomial B-splines for FDE problems. In particular, (locally) nonuniform knot sequences could be considered to improve accuracy for nonsmooth solutions. In this perspective, B-spline collocation methods are a problem-independent tool to face FDE problems and offer an appealing alternative to state-of-the-art methods such as the elegant collocation/Galerkin spectral methods for approximating the solution of (1) obtained by exploiting the connection between Jacobi polynomials and pseudo eigenfunctions of the Riesz fractional operator; see References 6 and 10 and references therein.

The spectral analysis in the present work will provide a strong guidance for forthcoming research. Indeed, the result in Theorem 6 is a key ingredient for studying the symbol of matrices arising from B-spline collocation methods for more general FDE problems. In particular, additional reaction and advection terms do not modify the symbol of the corresponding matrices; see Remark 9. Furthermore, FDE problems involving nonconstant coefficients can be addressed by applying the framework of GLT (Generalized locally Toeplitz) sequences.³⁵

Following the results in References 11,12,17,18, all the information provided by the symbol can be leveraged for the design of effective preconditioners and fast multigrid/multi-iterative solvers²⁰ whose convergence speed is robust with respect to the mesh size and the spline degree as well as the fractional derivative order; see also Remarks 7 and 8.

ACKNOWLEDGMENTS

This study does not have any conflicts to disclose. All authors are members of the INDAM research group GNCS. The last two authors are partially supported by the Beyond Borders Program of the University of Rome Tor Vergata through the project ASTRID (CUP E84I19002250005) and by the MIUR Excellence Department Project awarded to the Department of Mathematics, University of Rome Tor Vergata (CUP E83C18000100006). Open Access Funding provided by Università degli Studi dell'Insubria within the CRUI-CARE Agreement.

DATA AVAILABILITY STATEMENT

Data sharing is not applicable to this article as no new data were created or analyzed in this study.

ORCID

Mariarosa Mazza  <https://orcid.org/0000-0002-8505-6788>

Marco Donatelli  <https://orcid.org/0000-0001-7958-9126>

Carla Manni  <https://orcid.org/0000-0002-1519-4106>

Hendrik Speleers  <https://orcid.org/0000-0003-4110-3308>

REFERENCES

1. Bai J, Feng X. Fractional-order anisotropic diffusion for image denoising. *IEEE Trans Image Process.* 2007;16:2492–502.
2. Bueno-Orovio A, Kay D, Grau V, Rodriguez B, Burrage K. Fractional diffusion models of cardiac electrical propagation: role of structural heterogeneity in dispersion of repolarization. *J Royal Soc Interface.* 2014;11:20140352.
3. Ervin VJ, Roop JP. Variational formulation for the stationary fractional advection dispersion equation. *Numer Methods Partial Differ Equ.* 2006;22:558–76.
4. Hejazi H, Moroney T, Liu F. Stability and convergence of a finite volume method for the space fractional advection-dispersion equation. *J Comput Appl Math.* 2014;255:684–97.

5. Lin Z, Wang D. A finite element formulation preserving symmetric and banded diffusion stiffness matrix characteristics for fractional differential equations. *Comput Mech.* 2018;62:185–211.
6. Mao Z, Karniadakis GE. A spectral method (of exponential convergence) for singular solutions of the diffusion equation with general two-sided fractional derivative. *SIAM J Numer Anal.* 2018;56:24–49.
7. Meerschaert MM, Tadjeran C. Finite difference approximations for fractional advection-dispersion flow equations. *J Comput Appl Math.* 2004;172:65–77.
8. Tian W, Zhou H, Deng W. A class of second order difference approximations for solving space-fractional diffusion equations. *Math Comput.* 2015;84:1703–27.
9. Wang H, Du N. A superfast-preconditioned iterative method for steady-state space-fractional diffusion equations. *J Comput Phys.* 2013;240:49–57.
10. Zeng F, Mao Z, Karniadakis GE. A generalized spectral collocation method with tunable accuracy for fractional differential equations with end-point singularities. *SIAM J Sci Comput.* 2017;39:A360–83.
11. Donatelli M, Mazza M, Serra-Capizzano S. Spectral analysis and structure preserving preconditioners for fractional diffusion equations. *J Comput Phys.* 2016;307:262–79.
12. Donatelli M, Mazza M, Serra-Capizzano S. Spectral analysis and multigrid methods for finite volume approximations of space-fractional diffusion equations. *SIAM J Sci Comput.* 2018;40:A4007–39.
13. Lei SL, Sun HW. A circulant preconditioner for fractional diffusion equations. *J Comput Phys.* 2013;242:715–25.
14. Moghaderi H, Dehghan M, Donatelli M, Mazza M. Spectral analysis and multigrid preconditioners for two-dimensional space-fractional diffusion equations. *J Comput Phys.* 2017;350:992–1011.
15. Pan J, Ng MK, Wang H. Fast preconditioned iterative methods for finite volume discretization of steady-state space-fractional diffusion equations. *Numer Algor.* 2017;74:153–73.
16. Pang H, Sun HW. Multigrid method for fractional diffusion equations. *J Comput Phys.* 2012;231:693–703.
17. Donatelli M, Garoni C, Manni C, Serra-Capizzano S, Speleers H. Robust and optimal multi-iterative techniques for IgA collocation linear systems. *Comput Methods Appl Mech Eng.* 2015;284:1120–46.
18. Donatelli M, Garoni C, Manni C, Serra-Capizzano S, Speleers H. Symbol-based multigrid methods for Galerkin B-spline isogeometric analysis. *SIAM J Numer Anal.* 2017;55:31–62.
19. Mazza M, Manni C, Ratnani A, Serra-Capizzano S, Speleers H. Isogeometric analysis for 2D and 3D curl-div problems: spectral symbols and fast iterative solvers. *Comput Methods Appl Mech Eng.* 2019;344:970–97.
20. Serra-Capizzano S. Multi-iterative methods. *Comput Math Appl.* 1993;26:65–87.
21. Hofreither C, Takacs S. Robust multigrid for isogeometric analysis based on stable splittings of spline spaces. *SIAM J Numer Anal.* 2017;55:2004–24.
22. Hofreither C, Takacs S, Zulehner W. A robust multigrid method for isogeometric analysis in two dimensions using boundary correction. *Comput Methods Appl Mech Eng.* 2017;316:22–42.
23. Blank L. Numerical treatment of differential equations of fractional order. *Nonlinear World.* 1997;4:473–92.
24. Pedas A, Tamme E. On the convergence of spline collocation methods for solving fractional differential equations. *J Comput Appl Math.* 2011;235:3502–14.
25. Pitolli F. Optimal B-spline bases for numerical solution of fractional differential problems. *Axioms.* 2018;7:46.
26. Pitolli F. On the numerical solution of fractional boundary value problems by a spline quasi-interpolant operator. *Axioms.* 2020;9:61.
27. Xu K, Darve E. Isogeometric collocation method for the fractional Laplacian in the 2D bounded domain. *Comput Methods Appl Mech Eng.* 2020;364:112936.
28. Pezza L, Pitolli F. A multiscale collocation method for fractional differential problems. *Math Comput Simul.* 2018;147:210–9.
29. Liu J, Fu H, Wang H, Chai X. A preconditioned fast quadratic spline collocation method for two-sided space-fractional partial differential equations. *J Comput Appl Math.* 2019;360:138–56.
30. Donatelli M, Garoni C, Manni C, Serra-Capizzano S, Speleers H. Spectral analysis and spectral symbol of matrices in isogeometric collocation methods. *Math Comput.* 2016;85:1639–80.
31. Auricchio F, Beirão da Veiga L, Hughes TJR, Reali A, Sangalli G. Isogeometric collocation methods. *Math Models Methods Appl Sci.* 2010;20:2075–107.
32. Cai M, Li C. Regularity of the solution to Riesz-type fractional differential equation. *Integral Transf Spec Funct.* 2019;30:711–42.
33. Hao Z, Zhang Z. Optimal regularity and error estimates of a spectral Galerkin method for fractional advection-diffusion-reaction equations. *SIAM J Numer Anal.* 2020;58:211–33.
34. Podlubny I. *Fractional differential equations.* San Diego: Academic Press; 1998.
35. Garoni C, Serra-Capizzano S. *Generalized locally Toeplitz sequences: theory and applications.* Vol I. Cham: Springer; 2017.
36. Barbarino G, Serra-Capizzano S. Non-Hermitian perturbations of Hermitian matrix-sequences and applications to the spectral analysis of the numerical approximation of partial differential equations. *Numer Linear Algebra Appl.* 2020;27:e2286.
37. Grenander U, Szegő G. *Toeplitz forms and their applications.* 2nd ed. New York: Chelsea; 1984.
38. de Boor C. *A practical guide to splines.* Revised ed. New York: Springer-Verlag; 2001.
39. Lyche T, Manni C, Speleers H. Foundations of spline theory: B-splines, spline approximation, and hierarchical refinement. In: Lyche T et al., editors. *Splines and PDEs: from approximation theory to numerical linear algebra.* Lecture Notes in Mathematics. Volume 2219; Cham: Springer; 2018. p. 1–76.
40. Unser M, Blu T. Fractional splines and wavelets. *SIAM Rev.* 2000;42:43–67.

41. Chui CK. An introduction to wavelets. San Diego: Academic Press; 1992.
42. Garoni C, Manni C, Pelosi F, Serra-Capizzano S, Speleers H. On the spectrum of stiffness matrices arising from isogeometric analysis. *Numer Math.* 2014;127:751–99.
43. Speleers H. Inner products of box splines and their derivatives. *BIT Numer Math.* 2015;55:559–67.
44. Pan G, Chen W, Sze KY. Gauss-Jacobi-type quadrature rules for fractional directional integrals. *Comput Math Appl.* 2013;66:597–607.

How to cite this article: Mazza M, Donatelli M, Manni C, Speleers H. On the matrices in B-spline collocation methods for Riesz fractional equations and their spectral properties. *Numer Linear Algebra Appl.* 2022;e2462. <https://doi.org/10.1002/nla.2462>